Cell Stem Cell
Article

Highly Efficient miRNA-Mediated Reprogramming of Mouse and Human Somatic Cells to Pluripotency

Frederick Anokye-Danso,[1] Chinmay M. Trivedi,[2] Denise Juhr,[5] Mudit Gupta,[2] Zheng Cui,[1] Ying Tian,[1] Yuzhen Zhang,[1] Wenli Yang,[1,4] Peter J. Gruber,[3,4,5] Jonathan A. Epstein,[1,2,3,4] and Edward E. Morrisey[1,2,3,4,*]
[1]Department of Medicine
[2]Department of Cell and Developmental Biology
[3]Cardiovascular Institute
[4]Institute for Regenerative Medicine
University of Pennsylvania, Philadelphia, PA 19104, USA
[5]The Cardiac Center, Children's Hospital of Philadelphia, 34th Street and Civic Center Boulevard, Philadelphia, PA 19104, USA
*Correspondence: emorrise@mail.med.upenn.edu
DOI 10.1016/j.stem.2011.03.001

SUMMARY

Transcription factor-based cellular reprogramming has opened the way to converting somatic cells to a pluripotent state, but has faced limitations resulting from the requirement for transcription factors and the relative inefficiency of the process. We show here that expression of the *miR302/367* cluster rapidly and efficiently reprograms mouse and human somatic cells to an iPSC state without a requirement for exogenous transcription factors. This miRNA-based reprogramming approach is two orders of magnitude more efficient than standard Oct4/Sox2/Klf4/Myc-mediated methods. Mouse and human *miR302/367* iPSCs display similar characteristics to Oct4/Sox2/Klf4/Myc-iPSCs, including pluripotency marker expression, teratoma formation, and, for mouse cells, chimera contribution and germline contribution. We found that *miR367* expression is required for *miR302/367*-mediated reprogramming and activates *Oct4* gene expression, and that suppression of Hdac2 is also required. Thus, our data show that miRNA and Hdac-mediated pathways can cooperate in a powerful way to reprogram somatic cells to pluripotency.

INTRODUCTION

The transformation of differentiated cells to induced pluripotent stem cells (iPSCs) has revolutionized stem cell biology by providing a more tractable source of pluripotent cells for regenerative therapy. Although powerful, there are currently several limitations to iPSC generation, including the rather low efficiency of the process (0.2%–1.0%) and the necessity of forced expression of at least one pluripotent stem cell transcription factor, including Oct4, Nanog, Sox2, Klf4, and/or Myc. These limitations hamper the use of iPSC technology in high throughput formats such as generation of human iPSC clones from large patient populations.

The current standard strategy for iPSC generation relies upon ectopic expression of Oct4, Sox2, Klf4, and Myc (OSKM) (Takahashi and Yamanaka, 2006). Although there are several alternatives to some of these factors, including the use of other transcription factors, signaling factors, and pharmacological molecules, at least one pluripotent stem cell transcription factor—usually Oct4—is required for efficient iPSC reprogramming (Huangfu et al., 2008a, 2008b; Judson et al., 2009; Melton et al., 2010; Yoshida et al., 2009). Recently, several microRNAs (miRNAs) have been shown to enhance iPSC reprogramming when expressed along with combinations of the OSKM factors (Judson et al., 2009). These miRNAs belong to families of miRNAs that are expressed preferentially in embryonic stem cells and are thought to help maintain the ESC phenotype (Babiarz et al., 2008; Wang et al., 2007, 2008; Wang and Blelloch, 2009;). How these miRNAs enhance iPSC reprogramming is unclear but may have to do with their ability to regulate the cell cycle (Judson et al., 2009).

Of the miRNAs expressed at high levels in ESCs and iPSCs, the *miR302/367* cluster has been shown to be a direct target of Oct4 and Sox2 (Card et al., 2008), two of the critical factors required for iPSC reprogramming. Levels of *miR302/367* correlate with Oct4 transcripts in ESCs and early embryonic development, indicating an important role in ESC homeostasis and maintenance of pluripotency (Card et al., 2008). Despite their ability to enhance iPSC reprogramming in the presence of several of the OSKM factors (Judson et al., 2009), the ability of these miRNAs to directly reprogram somatic cells to an iPSC phenotype is unclear. We show that expression of the *miR302/367* cluster can directly reprogram mouse and human somatic cells to a pluripotent stem cell state in the absence of any of the previously described pluripotent stem cell transcription factors. Reprogramming by *miR302/367* is up to two orders of magnitude more efficient than that with the OSKM factors. We also show that valproic acid (VPA) is required for reprogramming mouse fibroblasts by specifically degrading Hdac2 protein, a finding that is supported by the efficient reprogramming of *Hdac2*$^{-/-}$ fibroblasts in the absence of VPA. Thus, the expression of *miR302/367* along with Hdac2 suppression allows for highly efficient iPSC reprogramming without the expression of the known reprogramming factors.

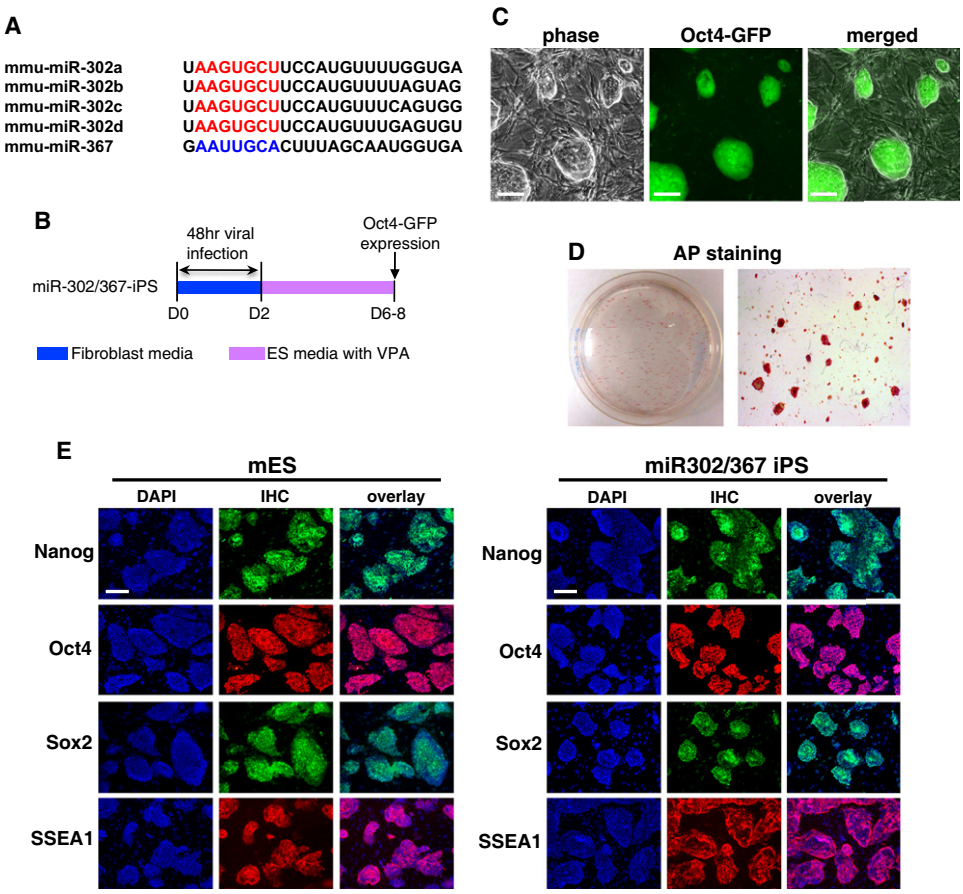

Figure 1. *miR302/367* Can Reprogram Mouse Fibroblasts to a Pluripotent Stem Cell Phenotype

(A) The sequences of the *miR302/367* cluster showing the similarity between members of the *miR302a/b/c/d* subfamily. *miR367* has a different seed sequence than *miR302a/b/c/d*.

(B) Schematic of viral expression protocol for *miR302/367* iPSC reprogramming with VPA. Day 0 is the start of viral transduction.

(C) *Oct4-GFP*-positive *miR302/367* clones at 7 days after starting viral transduction.

(D) AP staining of a primary induction plate of *miR302/367* iPSC clones at 8 days after starting viral transduction.

(E) Immunostaining for Nanog, Oct4, Sox2, and SSEA1 in both mouse ES and primary induction samples of *miR302/367* iPSCs at day 10, showing expression of pluripotent genes.

See also Figures S1 and S2. Scale bars, 100 μm.

RESULTS

miR302/367 Reprograms Fibroblasts to an iPSC Phenotype

Previous studies have shown that the *miR302/367* cluster comprises five miRNAs, four of which—*miR302a/b/c/d*—have identical seed sequences (Card et al., 2008; Figure 1A). The *miR302/367* cluster is located in intron 8 of the *Larp7* gene on chromosome 3 and is transcribed as a single polycistronic primary transcript (Card et al., 2008). The sequences of the *miR302/367* miRNAs are highly conserved across species (Card et al., 2008; Rosa et al., 2009). To determine whether expression of *miR302/367* could reprogram somatic cells, we generated a lentiviral vector, which expressed the 690 bp region encoding the mouse *miR302/367* sequences, and used it to transfect mouse embryonic fibroblasts (MEFs) derived from the *Oct4-GFP* mouse line (Lengner et al., 2007; Figure 1B). We included the Hdac inhibitor VPA in these experiments, as this has been shown to enhance iPSC reprogramming (Huangfu et al., 2008a). Surprisingly, we observed clones derived from *miR302/367*-transduced MEFs within 6 to 8 days after the start of a viral infection that had already assumed an ESC-like morphology (Figures 1C and 3A). Most of these clones were *Oct4-GFP* positive and alkaline-phosphatase positive (Figures 1C and 1D). These clones also expressed Nanog, Sox2, and SSEA1 (Figure 1E). In comparison, parallel expression of OSKM-expressing viruses in addition to VPA did not result in any visible clones until at least 8–10 days after starting viral transduction (Figure 3 and data not shown). Use of a polycistronic virus did not alter the timing or overall number of colonies generated by OSKM expression (data not shown and Sommer et al., 2009). Moreover, in the absence of VPA, *miR302/367* was unable to reprogram MEFs efficiently (see below and data not shown).

We further characterized the *miR302/367*-generated iPSC clones by microarray analysis for their similarity at the global

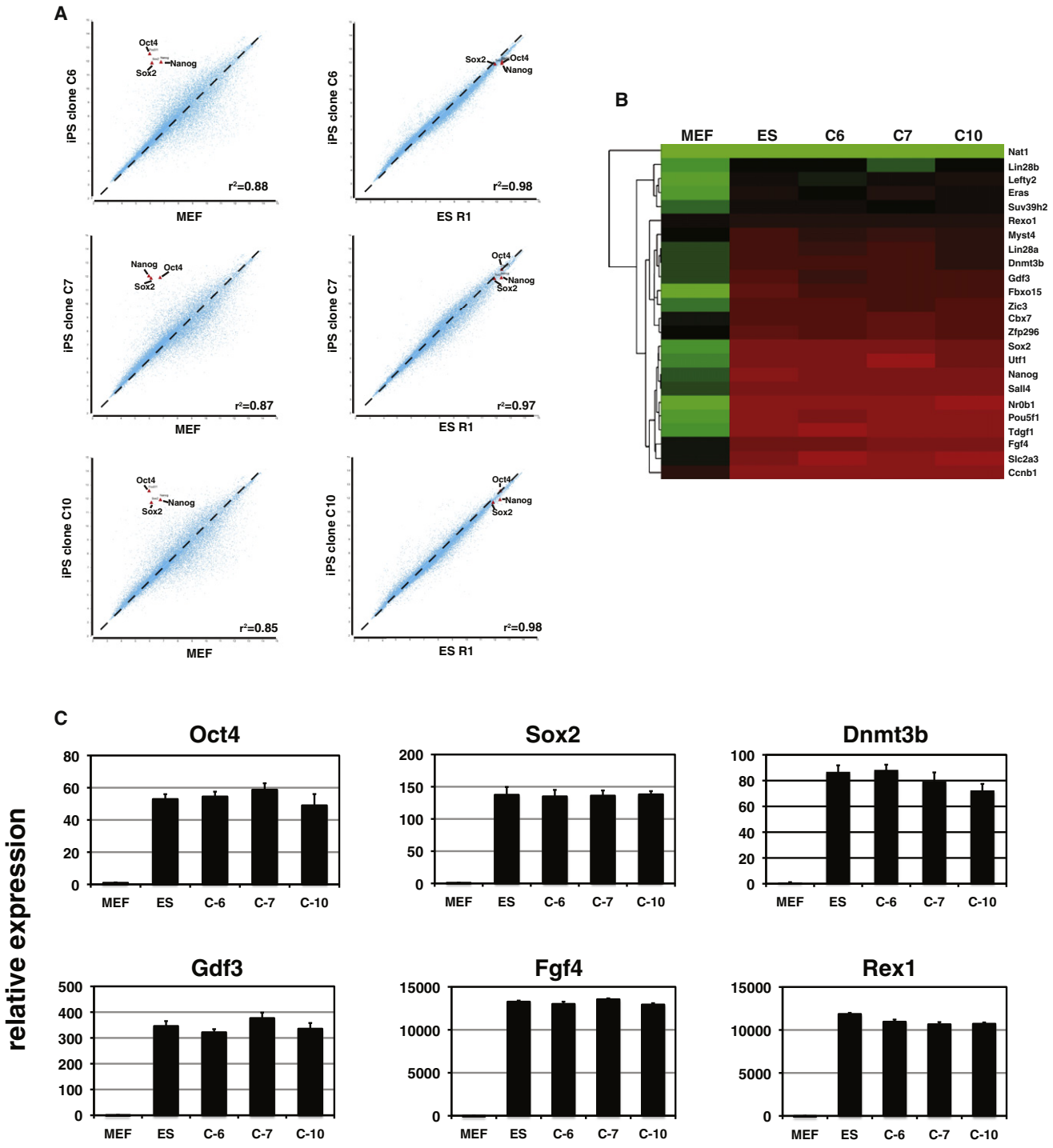

Figure 2. *miR302/367* iPSC Clones Have a Similar Expression Profile as Mouse ESCs

(A) Microarray experiments were used to show the similarity between *miR302/367* iPSC clones C6, C7, and C10 at passage 15 and the mouse ESC line R1.

(B) Heatmap of pluripotent gene expression of mouse ESC line R1 and *miR302/367* iPSC clones C6, C7, and C10 from experiment in (A).

(C) Q-PCR of pluripotent gene expression of *miR302/367* iPSC clones C6, C7, and C10 at passage 15 and mouse ESC line R1.

See also Figures S1 and S2.

gene expression level to the mouse ESC line R1. We used clones at passage 15 for these analyses. These data show a very high degree of correlation with global gene expression in the R1 ESC line (Figures 2A and 2B). These clones lacked integration of any of the OSKM factors that we use as controls, but did contain viral integration of the *miR302/367* lentivirus into the

genome (see Figure S1 available online). *miR302/367* iPSC clones that have been passaged serially maintain their ESC-like morphology and Q-PCR shows that they exhibit identical expression of pluripotent genes as mouse ESCs (Figure 2C and data not shown). Moreover, the *miR302/367* lentivirus is silenced at later passages (Figure S2). These results suggest that expression of *miR302/367* in addition to VPA was able to reprogram mouse MEFs to an iPSC state without expression of other previously described pluripotent factors.

miR302/367 Reprogramming is More Efficient Than OSKM Reprogramming

The rapid appearance of *miR302/367*-reprogrammed iPSCs suggested that expression of these miRNAs improved the temporal kinetics of reprogramming. To test this hypothesis, we expressed in parallel *miR302/367* and the OSKM genes using an identical number of starting MEFs and viral titer. VPA was included in both OSKM as well as *miR302/367*-reprogramming experiments. Previous studies have demonstrated that using the OSKM factors, an average colony-forming reprogramming efficiency of 0.2%–0.8% is observed (Huangfu et al., 2008a). Using *miR302/367*, we consistently observed *Oct4-GFP*-positive clones 7 days after starting viral transduction, which is sooner than cells transduced in parallel with the OSKM factors (Figure 3A). By counting the number of clones with ES-like morphology at 8 and 10 days after starting viral transduction, we show that expression of *miR302/367* produces two orders of magnitude more iPSC clones than when the OSKM factors are used (Figure 3B). At day 10, 79.8% of *miR302/367* iPSC clones exhibited robust expression of *Oct4-GFP*, which is greater than clones expressing the OSKM factors, of which only approximately 50% express *Oct4-GFP* (Figure 3C).

To better quantify this increase in iPSC reprogramming efficiency, we performed quantitative real-time PCR (Q-PCR) for pluripotent marker genes during the first 8 days of the reprogramming process on primary induction plates. The experiment used the same number of starting MEFs and viral titer for infection. These data indicate that while cells transduced with the OSKM factors expressed only very low levels of pluripotent marker genes during this time period, *miR302/367*-transduced cells expressed all of the genes examined at robust levels by day 8 (Figure 3D). The numbers of clones were such that after 8–10 days, the plates containing the *miR302/367* iPSC clones became overcrowded, resulting in decreased cell viability unless they were isolated and expanded. We also assessed the efficiency of reprogramming by *miR302/367* using fluorescence-activated cell sorting (FACS) for expression of GFP from the Oct4 locus in *Oct4-GFP* MEFs (Lengner et al., 2007). OSKM-reprogrammed MEFs do show *Oct4-GFP* expression at both 6 and 8 days of the reprogramming process, with up to 17% of cells expressing GFP by day 8, which is in the same range as previously reported (Figure 3E; Huangfu et al., 2008a). However, *miR302/367* is able to activate *Oct4-GFP* expression in up to 80% of MEFs after 8 days of reprogramming (Figure 3E). These data support the conclusion that *miR302/367* is able to reprogram fibroblasts to a pluripotent state up to two orders of magnitude more efficiently than OSKM factors.

miR302/367 iPSCs Can Generate Derivatives of Mesoderm, Endoderm, and Ectoderm in Teratomas; Generate Adult Chimeras; and Contribute to the Mouse Germline

To more fully characterize the pluripotent characteristics of *miR302/367* iPSCs, we generated teratomas in immune-deficient mice with multiple *miR302/367* iPSC clones. *miR302/367* iPSC-derived teratomas formed readily and exhibited tissues representing all three germ layers, as noted by structures resembling muscle fibers, keratinized epidermal cells, and luminal structures lined with gut-like epithelium (Figure 4A). Supporting these morphological findings, neural epithelial-like structures were positive for βIII-tubulin expression, muscle-like structures were positive for myosin heavy-chain expression, and gut-like epithelium was positive for E-cadherin expression (Figure 4B). A more stringent assay for pluripotency is determining whether *miR302/367* iPSCs can generate tissues within the developing embryo using chimeric embryo analysis. Therefore, we generated *miR302/367* iPSC clones from MEFs made from the *Rosa26lacZ* mouse line which expresses β-galactosidase ubiquitously (Friedrich and Soriano, 1991). Injection of these *miR302/367* iPSC clones generated high-percentage chimeras in more than 50% of the injected embryos (Figure 4C and data not shown). Most of these chimeras exhibited 80%–95% contribution from *miR302/367* iPSCs to all tissues examined (Figure 4C and Figure S3).

To test whether *miR302/367* iPSCs could contribute to the germline of mice, we injected three different mouse *miR302/367* iPSC clones derived from *Oct4-GFP* MEFs. Mouse gonads were collected at E13.5 and E15.5 and visualized both by whole-mount fluorescence and then fixed and sectioned for immunostaining for GFP expression. All three clones contributed efficiently to germ cells in the gonads of chimeric mice (Figures 4D–4J). Moreover, *miR302/367* iPSC clones generated from C57BL/6 MEFs can generate high-percentage postnatal chimeras, although germline transmission has not yet been examined (Figure 4K). Thus, *miR302/367* iPSC clones are pluripotent, are competent to generate all three germ layers, and contribute efficiently to the germline of mice. A summary of mouse clones tested for pluripotency is found in Table S1.

miR302/367 Can Reprogram Human Fibroblasts to a Pluripotent State More Efficiently Than OSKM Factors

To assess whether *miR302/367* can reprogram human fibroblasts, we transduced human foreskin and dermal fibroblasts with the *miR302/367* lentivirus. Within 12–14 days, we observed clones with the classic human ESC morphology (Figure 5A). Immunostaining of these clones showed they expressed OCT4, SSEA4, TRA-1-60, and TRA-1-81 (Figures 5B–5E). Q-PCR using three different *miR302/367* hiPSC cell clones shows that they all express pluripotent markers at levels equivalent to the hESC line HUES13 (Figure 5F). We reprogrammed the human foreskin fibroblast cell line BJ and performed DNA fingerprinting to show that clones from *miR302/367* reprogramming are derived from the original parental BJ line (Figure S4). Moreover, these human clones did not contain any integrants of the OSKM viruses, and the *miR302/367* virus was silenced in later passages (Figures S1 and S2). Interestingly, VPA was not required for reprogramming human fibroblasts and its addition

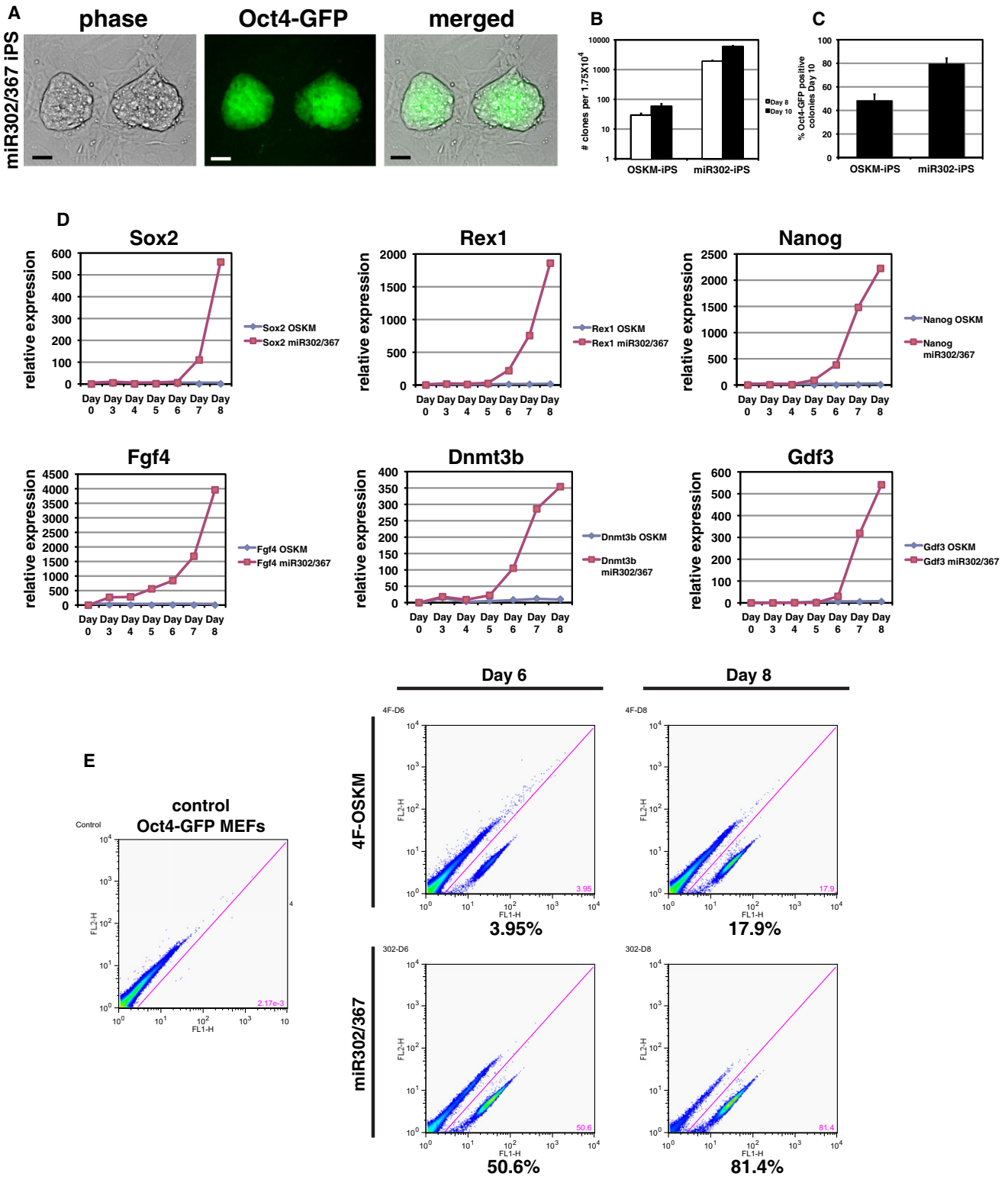

Figure 3. *miR302/367* Plus VPA is Two Orders of Magnitude More Efficient Than OSKM Factors in iPSC Reprogramming of Mouse Fibroblasts

(A) *miR302/367* iPSC clones are readily observed 6 to 7 days after starting viral transduction and express high levels of *Oct4-GFP* while OSKM-induced clones are not observed until 8–10 days, are very rare, and do not express significant levels of GFP from the *Oct4* locus.

(B) Counts of clones with ES-like morphology from transduction of 1.75 × 10^4 *Oct4-GFP* MEFs with equivalent amounts of either OSKM or *miR302/367* virus at 8 and 10 days after viral transduction. Data are the average of three assays ± SEM.

did not affect the efficiency of reprogramming (see below and data not shown). Teratomas were generated from seven different *miR302/367* hiPSC clones and all exhibited formation of mesoderm, endoderm, and ectoderm (Figures 5G–5L). A summary of human clones tested for pluripotency is found in Table S1.

We next assessed whether there was an increase in human reprogramming efficiency similar to what we observed in MEFs. Starting with the same number of human foreskin fibroblasts and OSKM and *miR302/367* viral titers, the number of colonies with ES-like morphology formed at 18 and 26 days after starting viral transduction is two orders of magnitude greater for *miR302/367* than when using OSKM expression (Figure 5M). Based on the cell counts, approximately 10% of human fibroblasts used for viral transduction produce iPSC clones (Figure 5M). Q-PCR from primary induction plates also reveals a dramatic increase in pluripotent gene expression in *miR302/367*-expressing versus OSKM-expressing human foreskin fibroblasts (Figure 5N). These data indicate that *miR302/367* can reprogram human as well as mouse fibroblasts to an iPSC state with greatly increased efficiency.

miR367 Expression is Required for *miR302/367* iPSC Reprogramming

The *miR302/367* cluster contains five different miRNAs, *miR302a/b/c/d* and *miR367*. All are expressed from a common promoter located in intron 8 of the *Larp7* gene (Card et al., 2008). *miR302a/b/c/d* all share a common seed sequence suggesting that they target a similar set of mRNAs and thus may act redundantly (Figure 1A). However, *miR367* has a different seed sequence and thus may target a different set of mRNAs (Figure 1A). Therefore, we tested whether *miR367* expression is required for *miR302/367* iPSC reprogramming. Using a lentivirus lacking the *miR367* sequence, we infected *Oct4-GFP* MEFs alongside the *miR302/367* lentivirus and assessed pluripotent reprogramming by colony counts, Q-PCR, and FACS analysis. The *miR302a/b/c/d* virus lacking *miR367* is expressed at high levels in MEFs (Figure 6A). However, *miR302a/b/c/d* did not generate any iPSC colonies when expressed in MEFs at day 10 of reprogramming (Figure 6B). Continued culture for up to 3 weeks did not result in formation of any iPSC colonies from *miR302a/b/c/d*-transduced MEFs (data not shown). Moreover, expression of *miR367* alone did not reprogram fibroblasts (data not shown). Q-PCR of primary induction plates 8 days after viral transduction shows that several important pluripotent genes were expressed at lower levels in *miR302a/b/c/d*-transduced MEFs versus *miR302/367*-transduced MEFs (Figure 6C). Importantly, *Oct4* expression is not observed at detectable levels in response to *miR302a/b/c/d* expression (Figure 6C, arrow). Using FACS analysis and *Oct4-GFP* MEFs, we show that there is no induction of *Oct4* gene expression when expressing *miR302a/b/c/d* without *miR367* while *miR302/367* expression induces robust *Oct4-GFP* expression by day 8 (Figure 6D). These data show that without *miR367* expression, *miR302a/b/c/d* expression was unable to reprogram mouse MEFs and that this correlated with a lack of induction of Oct4 gene expression. Thus, the coordinated action of the *miR302a/b/c/d* family along with *miR367* is required for iPSC reprogramming.

Low Levels of Hdac2 Permit *miR302/367* Reprogramming

Recent evidence has pointed to an important role for chromatin remodeling factors in regulating the ESC pluripotent state (Lagarkova et al., 2010; Mali et al., 2010). Previous data have shown that VPA, a known Hdac inhibitor, enhances OSKM reprogramming, suggesting an important role for Hdac-mediated chromatin remodeling in iPSC reprogramming (Huangfu et al., 2008a). We initially found that, in the absence of VPA, *miR302/367* was unable to efficiently reprogram MEFs to iPSCs and of the few clones that did develop, none survived clonal replating (Figures 7D and 7F and data not shown). Interestingly, VPA was not necessary for reprogramming of human foreskin or dermal fibroblasts (Figure 5). VPA has been reported to specifically degrade Hdac2 protein (Kramer et al., 2003). Therefore, we assessed whether expression of class I Hdacs was altered by *miR302/367* or VPA treatment by performing western blots for Hdac1, -2, and -3 expression during *miR302/367*-mediated reprogramming. While Hdac1 and Hdac3 expression levels were unchanged in all conditions, VPA caused degradation of Hdac2 protein in MEFs (Figure 7A). Expression of *miR302/367* did not affect the levels of Hdac1, -2, or -3 in the presence or absence of VPA in MEFs (Figure 7A). In contrast, human foreskin fibroblasts expressed much lower levels of Hdac2 protein, and the protein levels of Hdac2 were not affected by VPA in these cells (Figure 7B). These data suggest that low levels of Hdac2 may significantly enhance or even be required for *miR302/367* reprogramming and that human fibroblasts express much lower levels of Hdac2 than MEFs.

To test whether suppression of Hdac2 is specifically required for efficient reprogramming by *miR302/367*, we generated $Hdac2^{-/-}$ MEFs from $Hdac2^{flox/flox}$ mice using adenoviral-mediated cre excision of *Hdac2* and determined whether loss of Hdac2 altered the efficiency of *miR302/367* reprogramming of MEFs in the absence of VPA (Figure S5). We found that in $Hdac2^{-/-}$ MEFs transduced with the *miR302/367* virus, *Oct4-GFP*-positive clones were observed as early as 6 days post-viral infection (Figure 7C). Eight days after viral transduction, $Hdac2^{-/-}$ MEFs had formed significant numbers of iPSC clones in the absence of VPA, whereas wild-type MEFs in the absence of VPA did not generate any viable clones (Figure 7D). VPA addition to $Hdac2^{-/-}$ MEFs did not change the number of iPSC clones obtained (Figure 7D). The number of iPSC clones generated and the percentage of clones that were *Oct4-GFP* positive with *miR302/367*-transduced wild-type MEFs plus VPA and *miR302/367*-transduced $Hdac2^{-/-}$ MEFs lacking VPA were similar (Figure 7D and 7E). Loss of Hdac2 expression or VPA addition did not affect proliferation rates in MEFs

(C) Percentage of *Oct4-GFP*-positive clones 10 days after viral transduction with OSKM or *miR302/367*. Data are the average of three assays ± SEM.
(D) Q-PCR of the indicated pluripotent factors comparing OSKM versus *miR302/367* during the first 8 days after viral transduction.
(E) FACS analysis of *miR302/367*-reprogrammed *Oct4-GFP* MEFs compared to OSKM-reprogrammed MEFs at 6 and 8 days post-viral transduction. Scale bars, 50 μm.

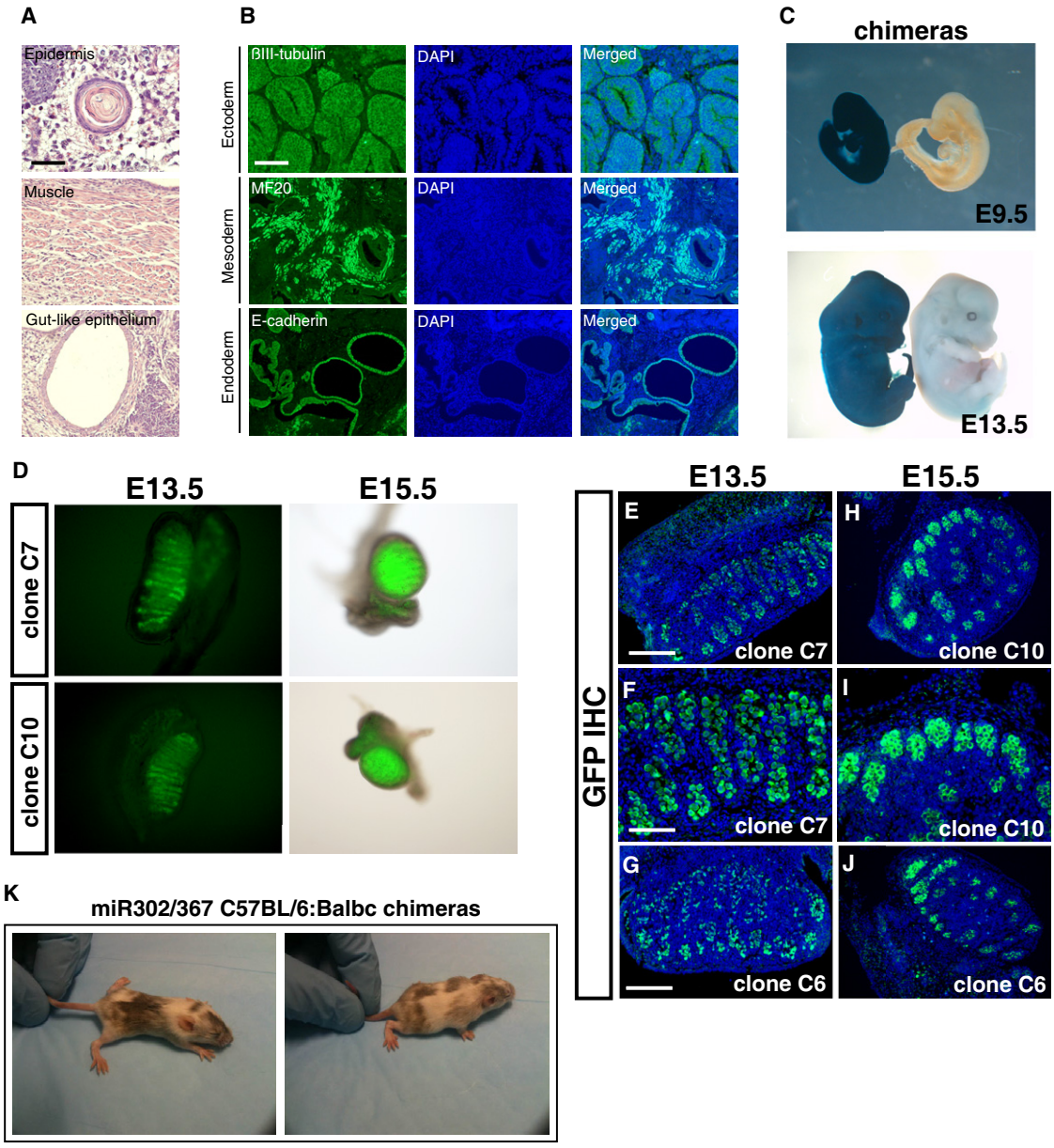

Figure 4. *miR302/367* iPSCs Can Generate Derivatives of Mesoderm, Endoderm, and Ectoderm and Contribute to the Germline of Mice

(A) Hematoxylin and eosin staining of teratomas derived from mouse *miR302/367* iPSC clones showing skin epidermal-like structures, muscle, and gut-like epithelium. These data are representative of five different *miR302/367* iPSC clones, all of which were injected and produced teratomas.

(B) Immunostaining of mouse *miR302/367* iPSC-derived teratoma tissues showing expression of βIII-tubulin-positive neural epithelium, MF20-positive striated muscle, and E-cadherin-positive endodermal cells.

(C) *miR302/367* iPSC clones can generate all tissues within the developing mouse embryo as shown by lacZ histochemical staining of high-percentage chimeric embryos derived from Rosa26-*miR302/367* iPSC clones at both E9.5 and E13.5.

(D–J) Both whole-mount fluorescence (D) and immunostaining for *Oct4-GFP* protein expression (E–J) show high-level contribution of *miR302/367* iPSC clones to the germline within the gonads of recipient mice. The data are representative of three clones (C6, C7, C10), which were injected into blastocysts and all three contributed to the germline.

(K) *miR302/367* iPSCs generated from C57BL/6 MEFs generate high-percentage postnatal chimeras as noted by coat color.

See also Figure S3. Scale bars: (A), 100 μm; (B, D, G, H, and J), 150 μm; (F and I), 100 μm.

(Figure S6). Q-PCR to assess expression of pluripotency-related genes also shows increased reprogramming by *miR302/367* in *Hdac2*$^{-/-}$ MEFs compared to wild-type MEFs without VPA (Figure 7F). Thus, low levels of Hdac2 or suppression of Hdac2 is required for efficient pluripotent stem cell reprogramming by *miR302/367*.

DISCUSSION

Current strategies for generating iPSCs rely upon expression of multiple pluripotent stem-cell-associated transcription factors. We show that a single miRNA cluster, *miR302/367*, can reprogram fibroblasts more efficiently than the standard OSKM method. With ongoing advances in miRNA biology, these findings may lead to a nonviral, nontranscription-factor mediated procedure for generating iPSCs for use not only in basic stem cell biology studies, but also for high throughput generation of human iPSC clones from large patient populations.

Previous studies have demonstrated the usefulness of iPSCs not only in the study of basic stem cell biology, but also in the ability to generate patient-specific iPSC clones, which can then be further differentiated into the cell lineage of choice, including hematopoietic, cardiomyocyte, and hepatocyte cell lineages (Moretti et al., 2010a, 2010b; Raya et al., 2010; Si-Tayeb et al., 2010). However, at this point the low efficiency of iPSC reprogramming is an impediment to adapting the process to high-throughput approaches. Such approaches would allow for the generation of iPSC clones from large patient populations obtained from genome-wide association studies for use in characterizing the identified genomic differences at the cell biological level. Our finding that reprogramming by *miR302/367* is up to two orders of magnitude more efficient than the OSKM factors suggests that this method may prove to be amenable for use in large-scale iPSC generation. Several other reports have demonstrated that using techniques including Sendai viral expression as well as direct transfection of synthesized mRNAs for the OSKM factors can improve the efficiency of iPSC reprogramming (Seki et al., 2010; Warren et al., 2010). Based on our data, we obtain efficiencies that are greater than either of these techniques, and using human fibroblasts, the percentage of cells that generate iPSC clones approaches 10%. Thus, *miR302/367* iPSC reprogramming is more efficient than previously described methods, including transfection of synthetic mRNAs for OSKM factors (Warren et al., 2010).

The mechanism underlying the increased efficiency of *miR302/367* iPSC reprogramming is likely to revolve in part around the nature of miRNA biology. First, miRNA expression does not require protein translation and thus leads to a fast response on protein expression based on inhibition of mRNA translation and stability. Second, miRNAs generally target scores or hundreds of mRNAs that coordinate expression of many different proteins, which can rapidly impose a dominant phenotypic change in cell identity. This ability to target many different mRNAs also simultaneously increases the complexity underlying the mechanism of *miR302/367* function. *miR302/367* collectively targets hundreds of different mRNA targets, including those that regulate chromatin remodeling and cell proliferation based on bioinformatic prediction algorithms (Betel et al., 2008; Grimson et al., 2007; Krek et al., 2005). Our data indicate that *miR367* expression is essential for iPSC reprogramming by the *miR302/367* cluster. As *miR367* has a different seed sequence, suggesting a different set of mRNA targets, analysis of the combinatorial regulation of *miR302a/b/c/d* and *miR367* targets may provide important information regarding both the pluripotent gene network and also factors whose expression is required to be suppressed for efficient iPSC reprogramming.

Our studies underscore the role of Hdac2 in iPSC reprogramming. The specific degradation of Hdac2 protein by VPA is likely the reason that this small molecule has been found to be more efficacious than other Hdac enzymatic inhibitors in enhancing iPSC reprogramming (Huangfu et al., 2008a). Several recent studies have demonstrated the importance of other chromatin remodeling processes in iPSC reprogramming (Bhutani et al., 2010; Lagarkova et al., 2010; Mali et al., 2010). Hdac2 has also been found to be part of an extended regulatory network for pluripotency in ESCs by interacting with both Oct4 and Myc (Kim et al., 2008). Since iPSC reprogramming involves the resetting of the epigenetic state of a differentiated cell to a pluripotent "ground state," additional studies into the necessity of chromatin remodeling will likely lead to better insight into cell lineage transdifferentiation events. Our finding that human cells, which express much lower levels of Hdac2 protein, do not require VPA for *miR302/367*-mediated reprogramming suggests that differing levels of Hdac2 may account, at least in part, for the different iPSC reprogramming efficiencies exhibited by different cell lineages. Moreover, Hdac2 expression may decline during development such that adult cells have little Hdac2 protein, resulting in the absence of an affect by VPA. Future studies into whether these correlations exist more broadly in other cell lineages may be beneficial for optimizing reprogramming by other methods including the OSKM factors.

Our studies show that miRNAs can be powerful tools for mediating iPSC reprogramming without the need for pluripotent factors including the OSKM factors. The current focus on developing miRNAs for therapeutic use could lead to a nonviral mediated method of altering *miR302/367* expression, which could in turn allow for a rapid miRNA/small molecule approach for iPSC reprogramming.

EXPERIMENTAL PROCEDURES

Lentiviral Vector Construction

A mouse genomic DNA fragment comprising *miR302/367* or *miR302a/b/c/d* family of miRNA was amplified by PCR using primers listed in Table S1. The amplified fragment was cloned into Acc65I and XhoI restriction enzyme sites of pENTR1A entry vector (Invitrogen) and verified by sequencing. The fragment was excised from the entry vector and ligated into BsrGI site of pLOVE destination vector (Blelloch et al., 2007) resulting in pLOVE-*miR302/367* vector. The pLOVE-*miR302a/b/c/d* vector was generated in the same fashion, but using a different 3′ primer that excluded the *miR367* sequence.

Cell Culture, Viral Production, and Induction of Pluripotent Stem Cells

Mouse fibroblasts were isolated from *Oct4-GFP*, *Rosa26-LacZ*, and *Hdac2$^{flox/flox}$* embryos at E13.5 and cultured in fibroblast medium as described (Takahashi et al., 2007). Hdac2 was excised by infection of *Hdac2$^{flox/flox}$* MEFs with adeno-cre virus. Human dermal fibroblasts were cultured in DMEM/F12, 15% FBS, penicillin/streptomycin, and L-glutamine. Viral particles were generated by transfection of plated 293T cells with pLOVE vectors encoding *miR302/367*, Oct4, Sox2, Klf4, or N-myc along with pMD.G and psPAX2 vectors as described (Blelloch et al., 2007). Supernatant from the transfected cells were collected every 24 hr for 48 hr and titered. The titered viral suspension was mixed with 0.5 μl of 10 μg/ml polybrene (American Bioanalytical, MA) per milliliter of viral suspension and used to infect fibroblasts. After viral infection, mouse fibroblasts were cultured in mouse ES medium supplemented with or without valproic acid at a final concentration of 2 mM for the indicated length of time. Infected human fibroblasts were cultured in human ES medium as described (Huangfu et al., 2008a; Takahashi et al., 2007).

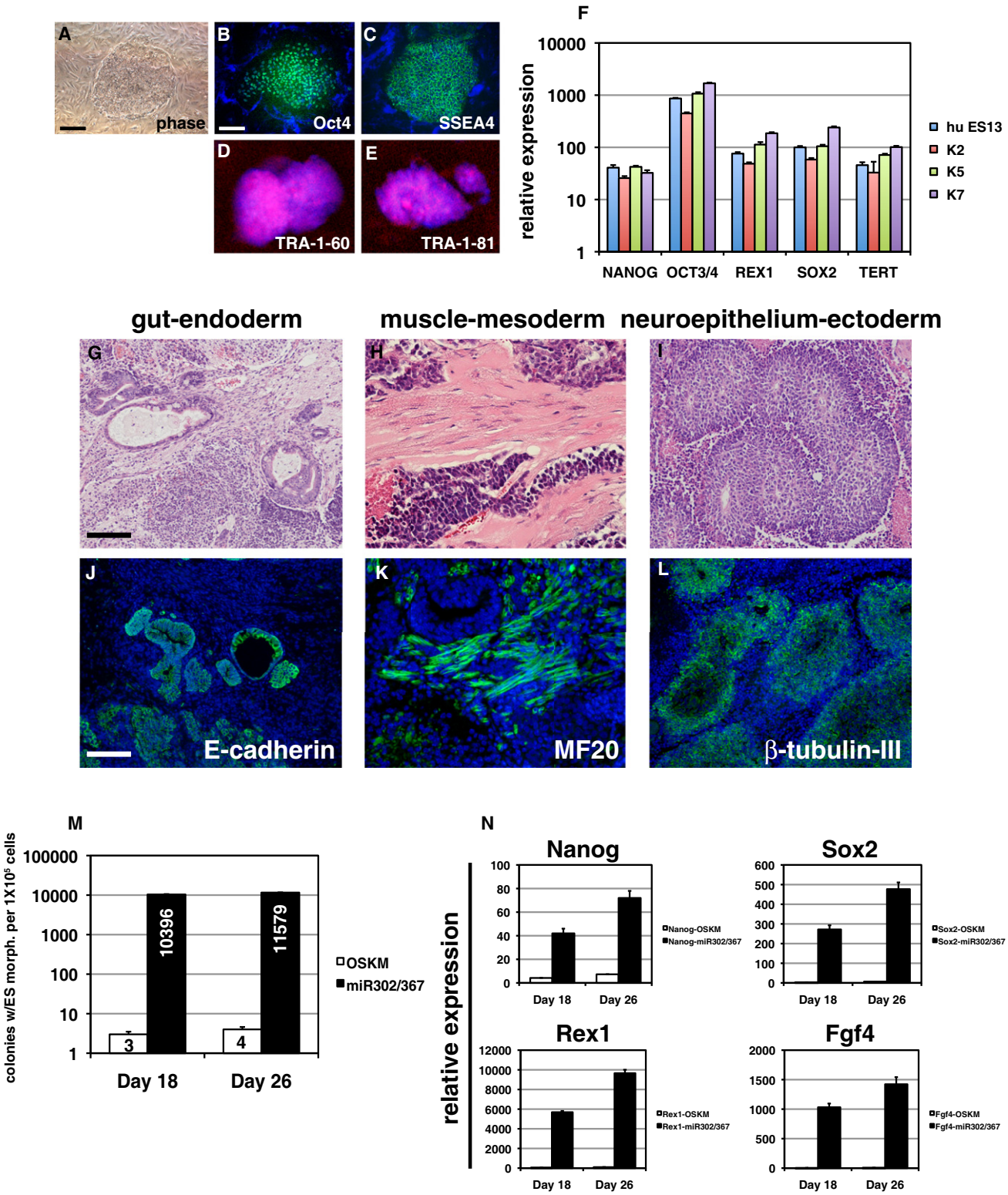

Figure 5. *miR302/367* Reprograms Human Fibroblasts to a Pluripotent State More Efficiently Than OSKM Factors

(A–E) Colony morphology and OCT4, SSEA4, TRA-1-60, and TRA-1-81 immunostaining of *miR302/367*-reprogrammed human fibroblasts.

(F) Q-PCR of pluripotent stem cell marker genes in three different *miR302/367*-reprogrammed human fibroblast lines as compared to the human ES line HUES13.

(G–I) Hematoxylin and eosin staining of teratomas derived from *miR302/367* human iPSC clones showing endoderm (gut)-, mesoderm (muscle)-, and ectoderm (neural epithelium)-like structures. These data represent the results from seven human *miR302/367* iPSC clones.

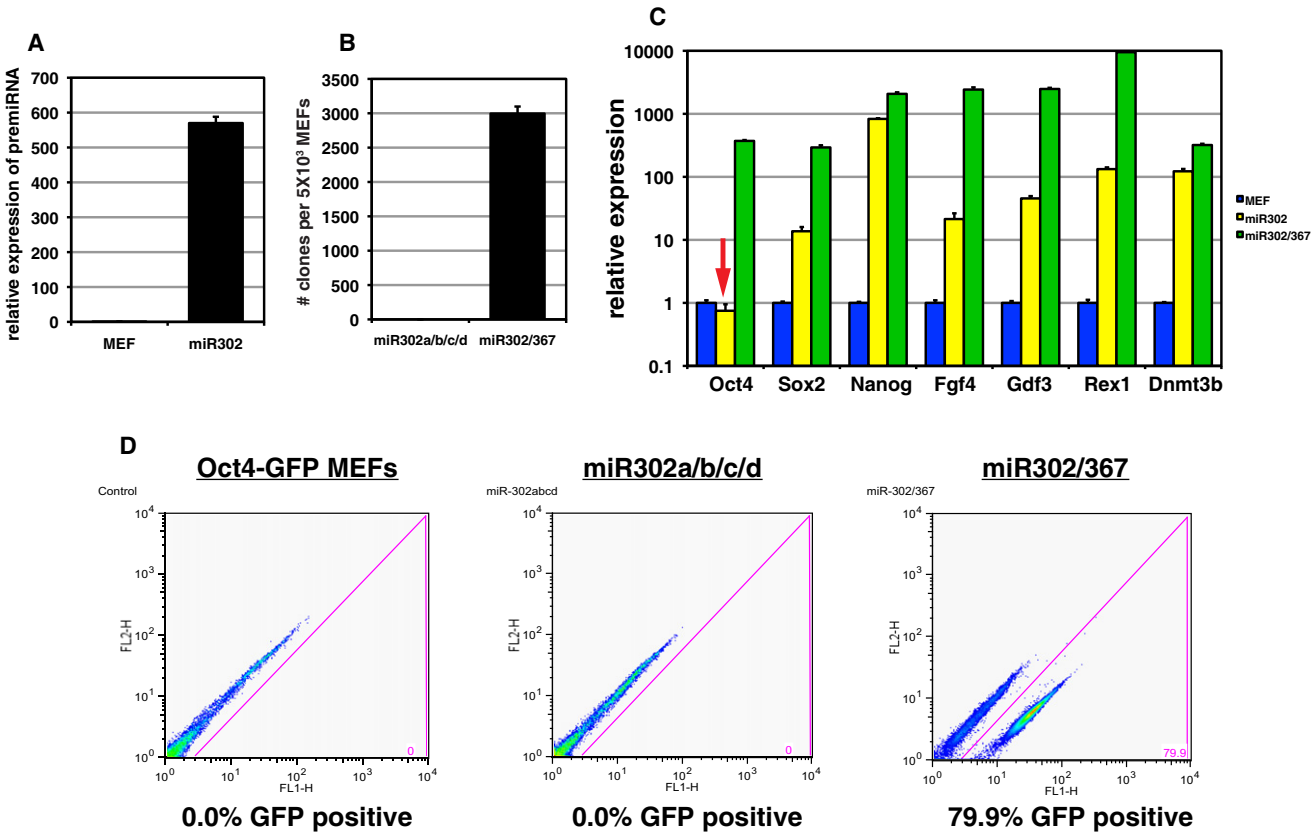

Figure 6. *miR367* Expression is Required for *miR302/367* iPSC Reprogramming

(A) The *miR302a/b/c/d* pre-miRNA is expressed at high levels in transduced MEFs.

(B) Number of colonies generated after 10 days of *miR302a/b/c/d* or *miR302/367* expression. Data are the average of four assays ± SEM.

(C) Pluripotent gene expression from primary induction plates 8 days after viral induction of *miR302a/b/c/d* or *miR302/367* viruses. Note lack of Oct4 gene expression in *miR302a/b/c/d*-expressing cells (red arrow). Data are the average of three assays ± SEM.

(D) FACS analysis of *Oct4-GFP* MEFs 8 days after transduction with either *miR302a/b/c/d* or *miR302/367* viruses.

Immunostaining

Clones were washed twice in PBS (with Mg^{2+} and Ca^{2+}) and fixed in 3.7% formaldehyde. Cells were permeabilized in 0.2% Nonidet P40 (Roche) and blocked in 10% goat serum. Cells were incubated in the following primary antibodies at 4°C overnight: Oct3/4 (Santa Cruz Biotechnology), Sox2 (R&D Systems), Nanog (Abcam), SSEA1 and SSEA4 (Developmental Studies Hybridoma Bank), TRA-1-60 and TRA-1-81 (Millipore, Inc.), and GFP (Clontech). Secondary antibodies are Alexa Fluor 488 and 568 (Invitrogen). The mounting medium used was Vectorshield with DAPI (Vector Laboratories). Alkaline phosphatase histochemical staining was performed using SIGMAFAST Fast Red TR/Naphtol AS-MX tablets following manufacturer's instructions (Sigma-Aldrich).

RNA Isolation, Quantitative RT-PCR, and Microarray Experiments

Total RNA was isolated using Trizol (Invitrogen). Two micrograms of RNA were used to synthesize cDNA using Superscript First Stand Synthesis Kit (Invitrogen). Real-time PCR was performed using SYBR Green (Applied Biosystems) by 7900HT Fast Real-Time PCR System (Applied Biosystems). Real-time primer sequences are listed in Table S1. For microarray experiments, the Affymetrix Mouse Gene 1.0 ST arrays were used. Microarray data were analyzed using Robust Multichip Analysis (RMA) and Principal Component Analysis (PCA) and the Partek Genomics Suite v6.5.

Teratoma Formation and DNA Fingerprinting Analysis

miR302/367 iPSCs were passaged twice on 0.1% gelatin-coated plates for an hour to remove feeders. A total of 5×10^5 cells were mixed with Matrigel and injected into each flank of NOD-SCID mice. Tumors were harvested at 4 weeks postinjection, fixed in 4% paraformaldehyde, and embedded in paraffin. Sectioned tumors were stained for hematoxylin and eosin. For immunofluorescence staining, the primary antibodies were βIII-tubulin (Abcam), MF-20 (Developmental Studies Hybridoma Bank), and E-cadherin (Cell Signaling). Genomic DNA from human *miR302/367* iPSC clones was used for DNA fingerprinting analysis (Cell Line Genetics, LLC, Madison, WI.).

Generation of Mouse Chimeras with *miR302/367* iPSC Clones

miR302/367 iPSCs were generated using *Rosa26-LacZ* mouse embryonic fibroblasts (Friedrich and Soriano, 1991). The cells were passaged twice on

(J–L) Immunostaining of *miR302/367* human iPSC-derived teratoma tissues showing expression of E-cadherin-positive endodermal cells, MF20-positive striated muscle, and βIII-tubulin-positive neural epithelium.

(M) Efficiency of *miR302/367* reprogramming in human foreskin fibroblasts by colony counts of clones with human ES-like morphology at 18 and 26 days postviral transduction. Data are the average of three assays ± SEM.

(N) Q-PCR of pluripotent gene expression in *miR302/367*-reprogrammed human foreskin fibroblasts at 18 and 26 days postviral transduction. Data are the average of three assays ± SEM.

See also Figures S1, S2, and S4. Scale bars: (A–E), 50 μm; (G–L), 150 μm.

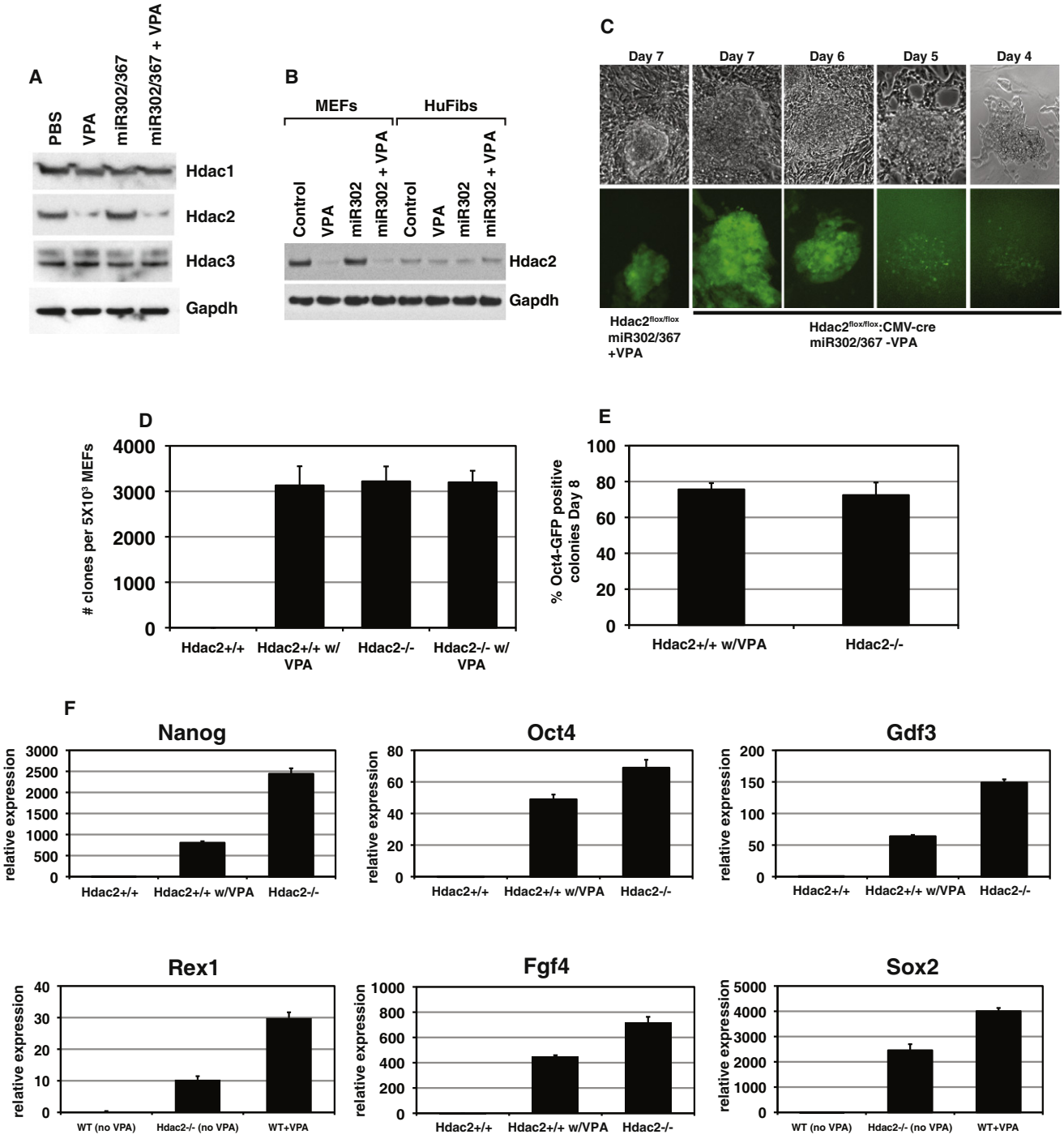

Figure 7. VPA Specifically Degrades Hdac2 Protein, and Suppression of Hdac2 is Required for iPSC Reprogramming by *miR302/367*

(A) VPA specifically degrades Hdac2, but not Hdac1 or Hdac3 proteins. Expression of *miR302/367* alone did not have any effect on Hdac1, -2, or -3 protein levels.

(B) Human foreskin fibroblasts express much lower levels of Hdac2 than MEFs.

(C) *Hdac2*$^{-/-}$ MEFs, in the absence of VPA, start to reprogram between 6 and 7 days postviral transduction, which is similar to wild-type MEFs treated with VPA.

(D) Number of clones generated with *Hdac2*$^{-/-}$ MEFs in the absence of VPA is similar to *Hdac2*$^{+/+}$ MEFs with VPA at 8 days postviral transduction. *Hdac2*$^{+/+}$ MEFs without VPA treatment did not generate any viable clones and VPA addition to *Hdac2*$^{-/-}$ MEFs did not increase the number of clones generated.

(E) Percentage of *Oct4-GFP*-positive clones is similar for *Hdac2*$^{+/+}$ MEFs with VPA treatment and *Hdac2*$^{-/-}$ MEFs without VPA treatment at 8 days postviral transduction.

(F) Q-PCR for pluripotent stem cell marker genes shows enhanced expression of pluripotency markers at day 8 of reprogramming by *miR302/367* in wild-type (*Hdac2*$^{+/+}$) and *Hdac2*$^{-/-}$ MEFs versus WT MEFs without VPA treatment. Data are the average of three assays ± SEM.

See also Figures S5 and S6.

0.1% gelatin-coated plates for an hour to remove feeders and injected into E3.5 C57BL/6 blastocysts. Embryos were harvested at E9.5 and E13.5 and stained for LacZ activity using previously described methods (Shu et al., 2002). For germline contribution experiments, *miR302/367* iPSC clones C6, C7, and C10, which were generated from *Oct4-GFP* MEFs, were used for blastocyst injections. Gonads were harvested from E13.5 and E15.5 embryos, visualized by fluorescence microscopy, and then fixed and sectioned for GFP immunostaining. Embryos and tissues were embedded in paraffin and sectioned as described (Cohen et al., 2009; Shu et al., 2002). All three clones contributed to the germline.

Western Blots

Total cell lysates were prepared for western blotting as previously described (Trivedi et al., 2008). Equal amounts of protein were resolved by SDS-PAGE and transferred to polyvinylidenedifluoride membranes. Membranes were incubated with Hdac1 antibody (1:1000 dilution, Cell Signaling), Hdac2 antibody (1:1000 dilution, Invitrogen), or Hdac3 antibody (1:1000 dilution, Sigma). Primary antibody binding was visualized by HRP-conjugated secondary antibody and detected by enhanced chemiluminescence (LumiGlo, Cell Signaling). For loading control, membranes were reprobed with primary antibody against GAPDH (1:2500 dilution, Abcam).

Proliferation Assays

Proliferation assays for MEFs were performed using the CellTiter 96 Aqueous One Solution Cell Proliferation kit (Promega, Inc.). Twenty microliters of CellTiter Reagent, which functions by being incorporated by viable cells into a colorimetric product that can be measured at 490 nm, was added to 100 μl of culture medium, incubated at 37°C, and absorbance was measured at 490 nm at 1.5 hr, 2.5 hr, and 4.5 hr.

Generation of Conditional *Hdac2$^{flox/flox}$* Mice

The *Hdac2$^{flox/flox}$* allele was generated by flanking exon 2 with *loxP* recombination sites using the targeting vector depicted in Figure S5A. Upon cre-mediated recombination, exon 2 is deleted and the resulting mRNA is out of frame with multiple early stop codons producing premature termination and loss of Hdac2 protein. This construct was electroporated into R1 ESCs; correctly targeted ES clones were identified using Southern blot analysis (Figure S5B) and used to generate high percentage chimeras and germline transmission of the *Hdac2$^{flox/+}$* allele. Ubiquitous CMV-*Cre* transgenic mice were used to delete Hdac2 and to demonstrate the resulting loss of Hdac2 protein by western blot analysis (Figure S4C). *Hdac2$^{flox/flox}$* mice were crossed with *Oct4-GFP* knock-in mice (Lengner et al., 2007) to generate *Hdac2$^{flox/flox}$*:*Oct4-GFP* mouse embryonic fibroblasts, which were treated with adenovirus-expressing cre recombinase to delete Hdac2 for reprogramming experiments.

SUPPLEMENTAL INFORMATION

Supplemental Information includes six figures, one table, and Supplemental Experimental Procedures and can be found with this article online at doi:10.1016/j.stem.2011.03.001.

ACKNOWLEDGMENTS

These studies were supported by funding from the NIH to E.E.M. (HL064632, HL087825, and HL100405), J.A.E. (HL071546 and HL100405), C.M.T. (HL098366), and an American Heart Association Jon Holden DeHaan Myogenesis Center Award to E.E.M. and J.A.E. The authors thank K. Zaret for the Rosa26-lacZ MEFs and gratefully acknowledge the support of the Penn Institute for Regenerative Medicine during these studies.

Received: September 8, 2010
Revised: February 2, 2011
Accepted: March 3, 2011
Published: April 7, 2011

REFERENCES

Babiarz, J.E., Ruby, J.G., Wang, Y., Bartel, D.P., and Blelloch, R. (2008). Mouse ES cells express endogenous shRNAs, siRNAs, and other Microprocessor-independent, Dicer-dependent small RNAs. Genes Dev. *22*, 2773–2785.

Betel, D., Wilson, M., Gabow, A., Marks, D.S., and Sander, C. (2008). The microRNA.org resource: targets and expression. Nucleic Acids Res. *36*, D149–D153.

Bhutani, N., Brady, J.J., Damian, M., Sacco, A., Corbel, S.Y., and Blau, H.M. (2010). Reprogramming towards pluripotency requires AID-dependent DNA demethylation. Nature *463*, 1042–1047.

Blelloch, R., Venere, M., Yen, J., and Ramalho-Santos, M. (2007). Generation of induced pluripotent stem cells in the absence of drug selection. Cell Stem Cell *1*, 245–247.

Card, D.A., Hebbar, P.B., Li, L., Trotter, K.W., Komatsu, Y., Mishina, Y., and Archer, T.K. (2008). Oct4/Sox2-regulated miR-302 targets cyclin D1 in human embryonic stem cells. Mol. Cell. Biol. *28*, 6426–6438.

Cohen, E.D., Ihida-Stansbury, K., Lu, M.M., Panettieri, R.A., Jones, P.L., and Morrisey, E.E. (2009). Wnt signaling regulates smooth muscle precursor development in the mouse lung via a tenascin C/PDGFR pathway. J. Clin. Invest. *119*, 2538–2549.

Friedrich, G., and Soriano, P. (1991). Promoter traps in embryonic stem cells: a genetic screen to identify and mutate developmental genes in mice. Genes Dev. *5*, 1513–1523.

Grimson, A., Farh, K.K., Johnston, W.K., Garrett-Engele, P., Lim, L.P., and Bartel, D.P. (2007). MicroRNA targeting specificity in mammals: determinants beyond seed pairing. Mol. Cell *27*, 91–105.

Huangfu, D., Maehr, R., Guo, W., Eijkelenboom, A., Snitow, M., Chen, A.E., and Melton, D.A. (2008a). Induction of pluripotent stem cells by defined factors is greatly improved by small-molecule compounds. Nat. Biotechnol. *26*, 795–797.

Huangfu, D., Osafune, K., Maehr, R., Guo, W., Eijkelenboom, A., Chen, S., Muhlestein, W., and Melton, D.A. (2008b). Induction of pluripotent stem cells from primary human fibroblasts with only Oct4 and Sox2. Nat. Biotechnol. *26*, 1269–1275.

Judson, R.L., Babiarz, J.E., Venere, M., and Blelloch, R. (2009). Embryonic stem cell-specific microRNAs promote induced pluripotency. Nat. Biotechnol. *27*, 459–461.

Kim, J., Chu, J., Shen, X., Wang, J., and Orkin, S.H. (2008). An extended transcriptional network for pluripotency of embryonic stem cells. Cell *132*, 1049–1061.

Kramer, O.H., Zhu, P., Ostendorff, H.P., Golebiewski, M., Tiefenbach, J., Peters, M.A., Brill, B., Groner, B., Bach, I., Heinzel, T., et al. (2003). The histone deacetylase inhibitor valproic acid selectively induces proteasomal degradation of HDAC2. EMBO J. *22*, 3411–3420.

Krek, A., Grun, D., Poy, M.N., Wolf, R., Rosenberg, L., Epstein, E.J., MacMenamin, P., da Piedade, I., Gunsalus, K.C., Stoffel, M., et al. (2005). Combinatorial microRNA target predictions. Nat. Genet. *37*, 495–500.

Lagarkova, M.A., Shutova, M.V., Bogomazova, A.N., Vassina, E.M., Glazov, E.A., Zhang, P., Rizvanov, A.A., Chestkov, I.V., and Kiselev, S.L. (2010). Induction of pluripotency in human endothelial cells resets epigenetic profile on genome scale. Cell Cycle *9*, 937–946.

Lengner, C.J., Camargo, F.D., Hochedlinger, K., Welstead, G.G., Zaidi, S., Gokhale, S., Scholer, H.R., Tomilin, A., and Jaenisch, R. (2007). Oct4 expression is not required for mouse somatic stem cell self-renewal. Cell Stem Cell *1*, 403–415.

Mali, P., Chou, B.K., Yen, J., Ye, Z., Zou, J., Dowey, S., Brodsky, R.A., Ohm, J.E., Yu, W., Baylin, S.B., et al. (2010). Butyrate greatly enhances derivation of human induced pluripotent stem cells by promoting epigenetic remodeling and the expression of pluripotency-associated genes. Stem Cells *28*, 713–720.

Melton, C., Judson, R.L., and Blelloch, R. (2010). Opposing microRNA families regulate self-renewal in mouse embryonic stem cells. Nature *463*, 621–626.

Moretti, A., Bellin, M., Jung, C.B., Thies, T.M., Takashima, Y., Bernshausen, A., Schiemann, M., Fischer, S., Moosmang, S., Smith, A.G., et al. (2010a). Mouse and human induced pluripotent stem cells as a source for multipotent Isl1+ cardiovascular progenitors. FASEB J. *24*, 700–711.

Moretti, A., Bellin, M., Welling, A., Jung, C.B., Lam, J.T., Bott-Flugel, L., Dorn, T., Goedel, A., Hohnke, C., Hofmann, F., et al. (2010b). Patient-Specific Induced Pluripotent Stem-Cell Models for Long-QT Syndrome. N. Engl. J. Med. *363*, 1397–1409.

Raya, A., Rodriguez-Piza, I., Navarro, S., Richaud-Patin, Y., Guenechea, G., Sanchez-Danes, A., Consiglio, A., Bueren, J., and Izpisua Belmonte, J.C. (2010). A protocol describing the genetic correction of somatic human cells and subsequent generation of iPSC cells. Nat. Protoc. *5*, 647–660.

Rosa, A., Spagnoli, F.M., and Brivanlou, A.H. (2009). The miR-430/427/302 family controls mesendodermal fate specification via species-specific target selection. Dev. Cell *16*, 517–527.

Seki, T., Yuasa, S., Oda, M., Egashira, T., Yae, K., Kusumoto, D., Nakata, H., Tohyama, S., Hashimoto, H., Kodaira, M., et al. (2010). Generation of induced pluripotent stem cells from human terminally differentiated circulating T cells. Cell Stem Cell *7*, 11–14.

Shu, W., Jiang, Y.Q., Lu, M.M., and Morrisey, E.E. (2002). Wnt7b regulates mesenchymal proliferation and vascular development in the lung. Development *129*, 4831–4842.

Si-Tayeb, K., Noto, F.K., Nagaoka, M., Li, J., Battle, M.A., Duris, C., North, P.E., Dalton, S., and Duncan, S.A. (2010). Highly efficient generation of human hepatocyte-like cells from induced pluripotent stem cells. Hepatology *51*, 297–305.

Sommer, C.A., Stadtfeld, M., Murphy, G.J., Hochedlinger, K., Kotton, D.N., and Mostoslavsky, G. (2009). Induced pluripotent stem cell generation using a single lentiviral stem cell cassette. Stem Cells *27*, 543–549.

Takahashi, K., and Yamanaka, S. (2006). Induction of pluripotent stem cells from mouse embryonic and adult fibroblast cultures by defined factors. Cell *126*, 663–676.

Takahashi, K., Tanabe, K., Ohnuki, M., Narita, M., Ichisaka, T., Tomoda, K., and Yamanaka, S. (2007). Induction of pluripotent stem cells from adult human fibroblasts by defined factors. Cell *131*, 861–872.

Trivedi, C.M., Lu, M.M., Wang, Q., and Epstein, J.A. (2008). Transgenic overexpression of Hdac3 in the heart produces increased postnatal cardiac myocyte proliferation but does not induce hypertrophy. J. Biol. Chem. *283*, 26484–26489.

Wang, Y., and Blelloch, R. (2009). Cell cycle regulation by MicroRNAs in embryonic stem cells. Cancer Res. *69*, 4093–4096.

Wang, Y., Medvid, R., Melton, C., Jaenisch, R., and Blelloch, R. (2007). DGCR8 is essential for microRNA biogenesis and silencing of embryonic stem cell self-renewal. Nat. Genet. *39*, 380–385.

Wang, Y., Baskerville, S., Shenoy, A., Babiarz, J.E., Baehner, L., and Blelloch, R. (2008). Embryonic stem cell-specific microRNAs regulate the G1-S transition and promote rapid proliferation. Nat. Genet. *40*, 1478–1483.

Warren, L., Manos, P.D., Ahfeldt, T., Loh, Y.H., Li, H., Lau, F., Ebina, W., Mandal, P.K., Smith, Z.D., Meissner, A., et al. (2010). Highly efficient reprogramming to pluripotency and directed differentiation of human cells with synthetic modified mRNA. Cell Stem Cell *7*, 618–630.

Yoshida, Y., Takahashi, K., Okita, K., Ichisaka, T., and Yamanaka, S. (2009). Hypoxia enhances the generation of induced pluripotent stem cells. Cell Stem Cell *5*, 237–241.